

Environmental-mediated relationships between tree growth of black spruce and abundance of spruce budworm along a latitudinal transect in Quebec, Canada

Angelo Fierravanti^{1,2}, Claudia Cocozza¹, Caterina Palombo¹, Sergio Rossi², Annie Deslauriers², Roberto Tognetti^{1,3}

¹ Dipartimento di Bioscienze e Territorio, Università degli Studi del Molise, Contrada Fonte Lappone, Pesche, I-86090, Italy

² Département des Sciences Fondamentales, Université du Québec à Chicoutimi, 555 boulevard de l'Université, Chicoutimi, QC-G7H2B1, Canada

³ The EFI Project Centre on Mountain Forests (MOUNTFOR), Edmund Mach Foundation, San Michele all'Adige, I-38010, Italy

Corresponding author: claudia.cocozza@unimol.it

Abstract

Changes in tree growth and insect distribution are projected due to climate warming. The expected effects of climate change on forest disturbance (e.g., insect outbreak) regime call for a better insight into the growth responses of trees to varying environmental conditions over geographical regions in eastern North America. In this study, the effects of a latitudinal thermal gradient and spruce budworm (SBW) outbreaks on the tree growth of black spruce (*Picea mariana* Mill.) were investigated along a 400 km transect from 48° N to 51° N across the continuous boreal forest in Quebec, Canada. Time series data were analyzed to synchronize climatic factors (temperature and precipitation trends), insect dynamics (SBW population frequency) and tree growth (ring-width chronology). Radial growth resulted as being synchronized with climate patterns, highlighting a positive effect of maximum temperatures on tree growth, especially in the northernmost site. Increasing temperatures and precipitation had a more positive effect on tree growth during epidemic periods, whereas the detrimental effects of SBW outbreaks on tree growth were observed with climate patterns characterized by lowered temperature. The lag between time series, synchrony and/or frequency of synchrony between tree growth and SBW outbreak were considered in order to link the growth of host trees and the dynamics of insect populations. The proposed analytical approach defined damage

severity on tree growth in relation to population dynamics and climate fluctuations at the northern distribution limit of the insect. Overall, a decline in tree growth was observed in these boreal forests, due to SBW outbreaks acting in combination with other stress factors.

Keywords: tree growth dynamics; insect population outbreaks; synchronicity analysis; climate change; black spruce

1. Introduction

In addition to the stressful conditions commonly experienced by boreal trees during extreme events, climate change is modifying disturbance regimes, increasing tree mortality and affecting species composition in boreal ecosystems (Candau and Fleming et al. 2011). In Canada, spruce budworm (*Choristoneura fumiferana* Clemens) (SBW) outbreaks cause recurrent growth declines of balsam fir (*Abies balsamea* L. Mill.), the main host of this defoliator (Boulanger et al. 2012). However, during epidemic periods, when the SBW population density is higher, other coniferous species, such as white spruce (*Picea glauca* Moench Voss), black spruce (*Picea mariana* Mill.) and red spruce (*Picea rubens* Sarg.), can also be severely defoliated (Simard et al. 2012). In spring, the feeding activity of the larvae is perfectly synchronized with balsam fir needle emergence. However, the currently increasing temperatures could advance insect and plant phenology, mismatching the synchronisms with balsam fir and making black spruce a more suitable host for SBW. This could modify the SBW target host, dramatically increasing the outbreak severity in the northern boreal zone, the black spruce domain, whereas the southern parts of the range would become too warm to sustain high SBW population levels (Régnière et al. 2012). In Quebec, Canada, three major SBW outbreaks occurred during the 20th century, in 1915–1929, 1946–1959 (Boulanger et al. 2012) and 1974–1988 (Boulet et al. 1996). The latter caused the defoliation of 55 million ha of black spruce stands. The first outbreak of the 21st century is still ongoing in eastern Canada, where the defoliated area has doubled every year since 2005. In 2012, more than 2 million ha of forest were affected (Direction de la protection des forêts 2012).

The SBW periodicity is defined by migrations and local population dynamics (Shlichta and Smilanich 2012). Jardon et al. (2003) studied this periodicity, synchronism and impact of SBW in Quebec, observing cyclical outbreaks occurring with frequency of 25–28 years at a supra-regional level and lasting 8 years or more (Jardon et al. 2003; Tremblay et al. 2011). Climate is the main factor that drives SBW dynamics, and the range of the outbreaks is predicted to shift beyond the traditional limits as the climate becomes more favorable (Bouchard and

Pothier 2010; Régnière et al. 2012; Zhang et al. 2014). Warmer winter temperatures can lead to overwintering survival, significantly increasing the abundance of insect populations (Han and Bause 2000), and longer summers in Eastern Canada may make northern sites more suitable for SBW attacks. The fluctuations in insect survival, caused by a poor synchronism between larval and bud phenology, seem to affect black spruce, whose bud flush is later than that of balsam fir and white spruce (Régnière et al. 2012). An increase in mean annual temperature of 2–5 °C across eastern Canada in the next 50 years, as projected by current climate models (Christensen et al. 2007), may induce phenological changes and trophic interactions among host trees, herbivorous insects and their natural enemies in boreal forests (Pureswaran et al. in press). Indeed, northern expansion of SBW in Quebec and climate-induced narrowing of the phenological mismatch between the insect and its secondary host may trigger more severe defoliation and mortality in black spruce forests.

Climatic factors play an important role in defining the severity and duration of outbreaks, as well as their synchrony (Gray 2008; Williams and Liebhold 2000). The degree of biological synchrony between host (black spruce) and parasite (SBW) depends on the overlap of the potential distribution of trees (as source of needles) and insect populations (Régnière et al. 2012). Therefore, the synchrony between tree growth and SBW dynamics is useful in order to understand the evolution and intensity of outbreaks, and the effect of severe infestation on stand productivity (Boulanger et al. 2012). Using the predictions of the effects of climate change on SBW outbreaks, models are required that describe how SBW defoliation dynamics interact with tree growth patterns across seasons and landscapes, and how they could affect the future productivity of forests (Krause et al. 2012). Moreover, Candau and Fleming (2011) found that the spatial distribution of past defoliation was related to winter and spring temperatures, and stand composition. However, the role of climate in determining the spatial and temporal distribution of defoliation caused by SBW and the interactions with stand productivity are still uncertain, as is the relative importance of the various causes of tree mortality (insect outbreaks vs. drought spells).

An innovative approach was applied in this paper, with the aim of examining the dynamics of black spruce growth in relation to the role of climatic factors in determining the severity and duration of SBW outbreaks, rather than reconstructing the history of SBW outbreaks using dendrochronology. We applied a mathematical function on time series data (Cocozza et al. 2012) to synchronize climatic factors (temperature and precipitation trends), insect dynamics (SBW populations), and tree growth (ring-width chronologies) obtained in black spruce stands along a latitudinal gradient in Quebec. We expected that 1) changes in monthly temperatures

and precipitation during the 20th century have progressively amplified the sensitivity of black spruce to SBW incidence, increasing synchrony between time series (tree rings and SBW outbreaks) and growth reduction during outbreaks, and 2) tree growth patterns have also varied along a latitudinal gradient under the influence of changing SBW synchrony, with growth of northern trees benefiting from warming and with greater phenological synchrony between black spruce and SBW in warmer sites.

2. Materials and methods

2.1. Study area

The study was conducted in black spruce stands from 48 to 51° N within the continuous boreal forest of Quebec, Canada (Fig. 1). The climate is subhumid-subpolar continental with mean annual temperatures ranging between -0.9 and 2.0 °C. The region has long winters with temperatures below zero, January being the coldest month with extremes of -47 °C, and short summers with maximum absolute temperatures exceeding 30 °C (Lugo et al. 2012). The landscape is characterized by glacial till deposits and an undulating morphology with many gently-sloping hills reaching 500–700 m a.s.l. (Rossi et al. 2011).

Four permanent sites were selected along a latitudinal gradient, Simoncouche (abbreviated as SIM) at the lowest latitude, Bernatchez (BER) at the highest altitude, Mistassibi (MIS), and Camp Daniel (DAN), the coldest site (Fig. 1) (Lugo et al. 2012).

2.2. Dendrochronological analysis

Fieldwork was carried out in summer 2013. In each site, the trees were selected to maximize the temporal and spatial extent of the time series. Care was also taken to select trees with canopies well separated from each other to reduce the effect of competition on tree growth. Two increment cores were extracted from 21 (SIM), 18 (BER and DAN) and 20 (DAN) black spruce trees with an increment borer 0.5 cm in diameter, at breast height (1.3 m) and at an angle of 120° from one another. Cores were mounted on channeled wood sticks, seasoned in a fresh-air dry store and sanded.

Tree ring widths (TRW) were measured to the nearest 0.01 mm using the LINTAB-measurement equipment at 60× magnifications. The Time Series Analysis Programme (TSAPWin) software package (Frank Rinn, Heidelberg, Germany) was used for statistical analyses on tree rings. TRW chronologies of each tree were cross-dated first visually and then statistically by the percentage agreement in the signs of the first-differences of the two time

series (the Gleichläufigkeit, Glk) (Kaennel and Schweingruber 1995). The Glk is a measure of the year-to-year agreement calculated as the number of times that two series show the same upward or downward trend relative to the previous year. With an overlap of 10 years, Glk becomes significant ($p < 0.05$) at 76% and highly significant ($p < 0.01$) at 87%. In this study, the analyzed time series were mostly longer than 50 years and cross dating was considered successful if Glk was higher than 60%. The statistical significance of the Glk (GSL) was also computed. In addition, the TVBP, a Student's t value, and the cross date index (CDI) were used to investigate the significance of the best match; acceptable comparability is assumed with t -value higher than 3, and values of $CDI > 10$ were considered as being significant. The TVBP is a statistical tool commonly used to compare and cross-date ring-width series, which determines the degree of correlation between curves and eliminates low-frequency variations within the time series as each value is divided by the corresponding 5-year moving average. The software ARSTAN was used to standardize individual chronologies, producing tree-growth index (TRI) chronologies for each study area (Cook et al. 1990). A spline function with a 50% frequency response of 32 years was fitted to each tree ring raw series, computed by dividing observed by expected values. Mean standard chronologies were then used to analyze climate–growth relationships.

Descriptive statistics were applied to compare key properties of each chronology and included mean sensitivity (MS) and tree ring width SD, useful to assess high-frequency variations; mean inter-series correlation (\bar{r}) for all possible pairings of tree ring series from individual cores over a common time interval (Briffa 1995); first order serial autocorrelation (AC), measuring the persistence retained before and after standardization and expressed population signal (EPS; Wigley et al. 1984), which was determined by calculating the chronology signal as a fraction of the total chronology variance, quantifies the degree to which a particular sample chronology portrays a hypothetically perfect chronology. An $EPS > 0.85$ is considered a generally acceptable threshold for reliable chronologies.

2.3. Climate and pupae frequency

A dataset of climate, including total precipitation (Pc), mean maximum temperature (Tx), mean minimum temperature (Tn), and instar pupae relative frequency (SBW) was obtained by the interpolation of the 100 weather stations closest to the study sites and adjusted considering the geographical coordinates of each site by means of BioSIM 10 - Canada 1901-2011 package (Régnière and St-Amant 2007; Anderson and Sturtevant 2011; Jobidon et al. 2015). BIOSIM

is a reliable tool that has been repeatedly tested (Anderson and Sturtevant 2011; Simard et al. 2011; Régnière et al. 2012; Sturtevant et al. 2013). The BioSIM database was used to determine the frequency and time of the SBW phenological phases (Régnière et al. 2014). The relative frequency of SBW instar pupae was used to determine the mortality of instar larvae. The average frequencies of pupae were used to represent the relative presence of this stage. Therefore, an increase in the frequency of pupae was assumed to correspond to a decrease in SBW mortality.

The epidemic and endemic periods were derived from the dendrochronological reconstruction of Boulanger et al. (2012), which represents a model exercise to determine the negative interval of SBW outbreaks during long-period trends. In time series analysis, it is essential to consider autocorrelation or serial correlation, defined as the correlation of a variable with itself over successive time intervals. Temporal autocorrelation of climate variables and SBW patterns was accounted ($p < 0.05$) and performed in JMP 11 (SAS Institute, Cary, NC). Autocorrelation increases the chances of detecting significant trends, even if they are absent. However, the autocorrelation was not removed from the standardized chronologies in order to preserve the outbreak signal (Boulanger and Arseneault 2004). Climate and SBW time series were not standardized to maintain the long-term signal of chronologies.

2.4. Climate, tree growth and SBW relationships

The influence of climate on tree growth was assessed using the BootRes package (Zang and Biondi 2013) in R environment (R Foundation for Statistical Computing, Vienna, Austria). The climate-growth relationship was studied by correlation function (CF) analysis using the climatic variables from June of the previous year to August of the current year as independent variables, and the four standard mean chronologies as dependent variables. In order to analyze time series lags and correlations, cross dating of curves was performed using TSAPWin and considering TRW as reference, and Pc, Tx, Tn or SBW (instar pupae frequency) as sample for every epidemic and endemic period. Time series curves, sorted in epidemic and endemic periods, were moved into TSAPwin to determine the Glk and GSL, considering time lags between 0 (no lag) and 5 years. The percentage of agreement between time series was calculated taking into account a minimum of 65% overlapping at lag of 5 years (a GSL threshold for maximum statistical significance).

2.5. Trend analysis

The trend detection in tree growth and environmental parameters at the four sites was considered. Pearson's correlation coefficient was used to determine significant relationships between the climatic variables and tree growth.

Mean rank differences (Kruskal and Wallis 1952) was performed using OriginalPRO 8 software, considering the non parametric distribution statistically significant when $p < 0.05$, in order to test the similarity of different samples (time series).

The Mann-Kendall test, nonparametric test for monotonic trends, provided indication of whether a trend exists and if the trend is positive or negative, using the Kendall R-statistical package (McLeod 2013; Tognetti et al. 2014). Subsequent calculation of the rank correlation coefficient, Kendall's tau, allowed the comparison of the strength of the correlation between two data series; tau ranges between -1 and 1 and measures the degree of similarity between ranks of pairs of chronologies. The resultant Mann-Kendall test statistic (S) indicated how strong the trends in ring width and environmental variables are and whether they are increasing or decreasing.

2.6. Synchronicity analysis

Long intervals of synchrony (> 4 years) between tree growth patterns and SBW population dynamics were taken into account in order to verify the timing of events, quantify the extent and strength of temporal and spatial variability in outbreak frequency and duration, determine the nature of population fluctuations, as well as the presence and strength of spatial synchrony. The synchronism between the trends of tree-ring width, climate and SBW during 1901-2011 (CID - complete interval derivative) was performed applying the derivative function approach on time-series data (Cocoza et al. 2012). The derivative analysis was conducted with TSAPWin software. The derivative of the function describes the best linear approximation with respect to time of the function for each chosen value. This analysis allowed the rate of variation of a function to be emphasized: when the derivative is positive the input function is increasing, otherwise the function is decreasing. Moreover, the higher the value of the derivative, the faster is the change in the value of the function. The derivative approach was used to study the length and frequency of synchronized intervals, in order to verify the occurrence of positive SBW outbreaks and negative tree growth.

Climate patterns were defined combining the derivative values of the climatic trends in CID, epidemic and endemic periods. The most frequent patterns were then correlated to tree growth and SBW trends in epidemic and endemic periods. The comparison of tree growth with climate

patterns and SBW derivative series was made computing Pearson correlation coefficients. Derivative functions were applied on the standardized time series.

3. Results

3.1. Time series patterns

Descriptive statistics of the mean standard chronologies of each study area were above the minimum significance ($Gl_k > 60$; $TVBP > 5$; $CDI > 10$). The statistical cross-dating between individual standard chronologies with the same latitude led to a 5% discard of the total cores, giving significant EPS values (> 0.85) in each site. TRW series spanned from 50 (SIM) to 133 (DAN) years with a mean tree age of 101 years. Common trends of tree growth were found in all sites, negative behaviors of series were particularly visible during the outbreaks in 1946-1959 and 1974-1988 (Fig. 2); the 2005-2012 outbreak is ongoing and has not been considered for further analysis. Mean TRW was 0.92 mm, ranging from 0.50, in the northern sites, to 1.89 mm, in SIM. Mean sensitivity and tree ring width SD were 0.115 and 0.51, respectively (Table 1).

The bootstrapped correlation coefficients were significant for total precipitation in December of the previous year for BER and MIS, and in May of the current year for DAN (Fig. 3). Total precipitation was not significant for SIM (Fig. 3). Mean Tx and Tn affected tree growth, especially in DAN, showing a positive significant correlation with most of the spring and summer months of the current year (April, June and July). Mean Tx and Tn of December of the previous year also correlated positively with tree growth in DAN (Fig. 3).

Time lags between time series were found in endemic and epidemic periods with values from +1 to +5 years (Gl_k ranged between 56 and 92); whereas, no lags (0) were found in some cases (Gl_k ranging between 57 and 83) (Table 2). High values ($GSL > 95\%$) of statistical significance of time lags were found between tree growth and SBW in endemic periods (Table 2).

Mann–Kendall test showed a significant decreasing trend of TRW in all sites ($p < 0.01$) (Table 3). Significant increasing trends of Pc and Tn were found in all sites ($p = 0.001$); a significant increasing trend of SBW was found in SIM ($p = 0.001$); instead, a significant increasing trend of Tx was found in MIS ($p = 0.001$), and a significant decreasing trend of Tx in BER ($p = 0.01$) (Table 3).

Patterns of climatic variables were obtained by the combination of increasing or decreasing trends of the variables considered (Table 4). The frequency of each climate pattern was defined for CID, endemic and epidemic periods. The most frequent climate patterns were defined by: increase of Pc, Tx and Tn, with values of synchrony frequency of 24, 25, and 23% in CID,

outbreak and non-outbreak intervals/periods, respectively (pattern A); decrease of Pc and increase of Tx and Tn, with synchrony frequency of 20, 19, and 20% in CID, outbreak and non-outbreak periods, respectively (pattern B); increase of Pc and decrease of Tx and Tn, with synchrony frequency of 20, 21 and 10% in CID, outbreak and non-outbreak periods, respectively (pattern F); decrease of Pc, Tx and Tn, with synchrony frequency of 22, 21 and 23% in CID, outbreak and non-outbreak periods, respectively (pattern H) (Table 4).

3.2. Synchronicity output

According to the results of the homogeneity test (Kruskal-Wallis test), non-significant differences were found between time series (Table 3), indicating a similarity between TRW time series and each environmental variable. Greater synchrony was recorded between TRI and Tx for non-outbreak periods in the intervals 1928-38 and 1995-2003 for SIM, 1923-31 and 1907-16 for BER, and 1910-20 for DAN (these results were determined as shown for SIM in Fig. 4, for the sake of representativeness). Synchrony was also observed between TRI and Tn in 1912-21 for DAN, between TRI and Tn, and Tx, in 1964-71 for MIS, and Pc in 1964-71 for DAN (data not shown). This analysis highlighted synchrony and asynchrony periods, as the correspondence of increasing TRI with increasing SBW and vice versa, and detecting time lags between TRI and SBW, as reported in Figure 4 for SIM (as an example for all sites). High frequency was recorded for synchrony intervals from 1 to 6 years, for all the variables. The intervals of 2 and 3 consecutive years were the most representative for the synchrony of TRI with Pc, Tx and Tn, while intervals of 2 and 4 consecutive years were relevant in the case of the synchrony of TRI with SBW (instar pupae frequency) (Fig. 5).

Pearson's correlation showed significantly different relationships between TRI and climatic variables and SBW at each site, as defined by the relative mean frequency of synchronization (Table 3). Relationships between climate patterns and TRI and SBW (instar pupae relative frequency) were defined in CID (Table 5). Patterns showed high synchrony percentage in the considered intervals; however, plant-insect patterns did not always change with the same outline. Patterns of increasing TRI and SBW were detected with higher frequency in the outbreak periods. Patterns of increasing TRI and decreasing SBW were observed in the three considered intervals, as well as patterns of decreasing TRI and increasing SBW. Instead, patterns of decreasing TRI and SBW were more frequent in epidemic periods, in the climate pattern B (Table 5).

4. Discussion

4.1. Tree growth and climate responses

The growth of black spruce responded positively to increasing precipitation during the growing season and temperature in spring (Fig. 3). Tree-ring width was synchronized with climate patterns, highlighting a positive effect of maximum temperatures on the growth of black spruce, especially in the northernmost site (DAN) (Table 3). The controlling role of water availability and heat accumulation for radial increments in conifers of the eastern Canadian boreal forest has previously been documented (Genries et al. 2012; Drobyshev et al. 2013). Air temperature plays an important role in triggering the onset of spring photosynthesis in boreal conifers, which may affect the overall tree carbon assimilation (Tanja et al. 2003). In the same populations, Rossi et al. (2014) found that warmer sites had earlier onset and later ending of growth, resulting in longer durations and higher intensity of cell production. Moreover, high spring temperatures can also advance soil thawing for the growth resumption, resulting in an earlier availability of water for roots (Goodine et al. 2008). By contrast, a reduction in the period and amount of xylem production along the thermal gradient is associated with both later resumptions of growth in spring and earlier conclusions of xylem differentiation in autumn (Rossi et al. 2007).

A positive effect of increased summer precipitation was observed on tree growth of the following year (Fig. 3). Instead, high temperatures in later summer negatively affected the growth of black spruce the following year, by enhancing stand evapotranspiration and water deficit. The period of wood production, from mid-May to the end of August, likely benefits from a combination of late season increase in water availability and summer warmth, particularly at high latitudes (Ko Heinrichs et al. 2007). Nevertheless, the influence of temperature on the cambial activity of Norway spruce changes during the year, with a culmination in early spring (Gričar et al. 2007). At the same sampling sites as the current study, the onset of xylem growth in black spruce occurred from late May to mid-June (DOY 146-169), covering a range of more than 20 days (Rossi et al. 2011); the ending of xylem growth varied by more than a month, from early September in DAN and MIS to early October in SIM. Rossi et al. (2011) estimated longer durations of xylogenesis at higher temperatures, with increases of 8–11 days °C⁻¹ and a lengthening of 25% with a 3 °C increase in mean annual temperature, with potentially larger tree rings and stand productivity. Nevertheless, our results showed a tree growth decline in these boreal forests, regardless of the rising atmospheric CO₂ levels during the past century. Trees growing on these thin and unstructured soils might suffer from drought stress and nutrient limitation (Silva et al. 2010), which add to SBW disturbance.

A longer period for primary and secondary tree growth can result in disproportional resource requirements, particularly at lower latitudes of the closed black-spruce forest. If water supply is not sufficient to sustain evaporative demand, because saturation vapor pressure increases exponentially with increasing temperature, vapor pressure deficit increases exponentially when temperature increases and absolute humidity remains constant (Centritto et al. 2011). Consistent growth decreases or minor growth changes have been forecast in southern forest stands of Quebec (below 49° N) by modeling studies (Huang et al. 2013). At these latitudes, a significant amount of the precipitation generally falls in the form of rain in summer, allowing relatively constant water availability during the growing season. Although no detrimental decrease of soil water availability has been observed in the studied area (Rossi et al. 2014), and the occurrence of drought-induced reduction in xylem growth has been considered unlikely in black spruce (Krause et al. 2010; Belien et al. 2012), the southern closed boreal forest may experience water stress and composition shift with warming over time.

4.2. Relationships between tree growth and climate and SBW

Increases of temperature and precipitation (climate pattern A, Table 4) had more positive effects on tree growth during the epidemic periods (Table 5). The positive effect of warm summer temperature and late season precipitation on tree radial growth probably decreased the susceptibility of black spruce to insect damage in SBW outbreaks, as shown in the plant-insect pattern defined by increasing trends of tree growth and SBW (instar pupae frequency). However, Simard et al. (2008) found that carbon isotope enrichment and tree ring width decreased synchronicity in *A. balsamea* and *P. mariana*, which strongly supports a photosynthetic compensation induced by defoliation. Consequently, foliage availability might have sustained insect feeding and oviposition. This would have substantially increased the number of potential offspring of the following generation. Instead, the role of precipitation in winter was limited, mainly falling as snow that only melts successively.

Tree growth reduction induced by SBW outbreaks was comparable to previous studies (e.g., Kneeshaw et al. 2011). They showed more intense growth declines in correspondence to mid-century outbreaks than at the beginning and end of the century (e.g., Jardon et al. 2003). The effect of SBW increasing trend on the tree growth decline was observed when climate patterns F and H occurred (Table 5). This may suggest a different damage severity in relation to population dynamics and climate fluctuations at the northern distribution limit of the insect, and the eventual shift of SBW feeding preferences towards other primary producers (Gray 2008).

Alternating synchronous or asynchronous time series highlighted a temporal lag in the response of tree growth to SBW outbreaks, which induced a marked reduction in tree growth during the following year. This may be misleading about the harmfulness of SBW infestations in the current year and on projecting a negative trend in black spruce growth. However, an ecological link between host tree growth and insect population dynamics does exist and, in the long term, may evolve towards an altered frequency of SBW outbreaks in association with changes in climate and other external factors affecting black spruce.

The derivative analysis of synchronous cycles in tree growth trends and insect population dynamics suggests repeated and rapid SBW outbreaks, inducing marked growth reductions. The excessive feeding on buds and foliage produced a distinctive tree-ring signal. Consequently, a cyclic decrease of the insect population might be triggered by a hunger induced migration of moths to neighboring stands. Tree-ring studies in eastern Canada have shown that large SBW outbreaks usually develop over several years, and may expand from epicenters becoming less suitable for SBW (Jardon et al. 2003). However, the identification of SBW outbreaks did not always involve an impact on black spruce growth in the current year (Fig. 4). A delay in tree growth reduction was observed with lags from 1 to 4 years (Table 2), suggesting an effect of SBW outbreak on tree growth after the outbreak period when the insect population was decreasing. It may be assumed that the SBW outbreak was not immediately visible but that the insects brought about a progressive deterioration of the tree health after 3-4 years. SBW showed short (1-2 years) and negative intervals of synchrony, defined by simultaneous decreasing of the tree growth and SBW (instar pupae frequency) after four years, when food resources were exhausted. This implies that insect population dynamics may further differentiate tree growth patterns, in association with climate driven-factors (Gray 2008).

The lag between time series has been debated in the last decade, synchrony and/or frequency synchrony being observed between tree growth and SBW outbreak (Jardon et al. 2003; Boulanger and Arseneault 2004). It has been suggested that lags are based on growth patterns, e.g., the growth reduction in mature trees did not necessarily occur during the first year of a moderate to severe defoliation, which appears earlier in the upper canopy and depends on tree height (e.g., Krause et al. 2012). The branches can be defoliated at different intensity and times, resulting in a gradual loss of biomass and, consequently, a marked reduction in secondary growth and tree-ring width (Krause et al. 2012).

Generally, stand characteristics (forest type, stand structure, tree age, etc.) in the insect inventory can vary between locations, leading to incomplete assessment of insect disturbances and dynamics (Cooke and Roland 2007). Spatial and temporal factors affect outbreak dynamics

in forest ecosystems, inducing an overestimation of defoliated areas or species (Huang et al. 2008). Careful identification of synchrony between the growth of host trees and the occurrence of SBW outbreaks might provide valid information in order to expand the insect inventory database and tree disturbance responses at temporal and spatial scales. This approach will be useful in evaluating tree growth responses to climate and potential divergences. In the far north, weather stations are typically sparse, and often located some distance from and at different elevations than the tree-ring sites, which can cause decoupling of climatic conditions between the tree-ring sites and weather stations, making comparisons and homogenization difficult (D'Arrigo et al. 2008).

5. Conclusions

Tree growth in boreal forests was subjected to the additive interaction of SBW recurrent outbreaks with the environment. The synchronization of tree-ring chronologies with insect outbreaks provided a practical tool for the reconstruction of pest events and plant responses, as proxy for population dynamics. The assessment of the temporal and spatial variability of events was demonstrated to be useful in determining the frequency of SBW outbreaks and interactions with other disturbances, as well as the presence and strength of spatial autocorrelation, and describing the nature of population fluctuations. Increasing temperature and precipitation had more positive effects on tree growth in epidemic periods. Warm summer temperature and late season precipitation favored radial growth, probably decreasing the susceptibility of black spruce to insect damage during outbreaks.

This approach combining black spruce growth patterns and SBW population dynamics can help to disentangle the external forces, namely ongoing climate change, regulating periodicity and variability in time and space of insect outbreak regimes. In order to reduce the uncertainty in regional predictions, models using climate indexes at the global scale could incorporate the synchronization analysis of population dynamics and local drivers in Eastern Canada. Although the results are specific to black spruce and SBW in Quebec, we expect that a synchronization analysis of time series (climate patterns, tree growth and defoliation cycles) will be equally useful in explaining temporal fluctuations and defining hazard rates in other areas and on different trees, caused by outbreaks of other insect species.

ACKNOWLEDGEMENTS

The authors thank A. De Cristofaro and F. Lombardi (Università degli Studi del Molise) for their suggestions on insect traits and dendrochronology, and A. Garside for editing the English text. The research is linked to activities conducted within the COST FP1106 (STReESS - Studying Tree Responses to extreme Events: a SynthesiS).

REFERENCES

- Anderson, D.P., Sturtevant, B.R., 2011. Pattern analysis of eastern spruce budworm *Choristoneura fumiferana* dispersal. *Ecography* 34, 488-497.
- Belien, E., Rossi, S., Morin, H., Deslauriers, A., 2012. Xylogenesis in black spruce subjected to rain exclusion in the field. *Can. J. For. Res.* 42, 1306–1315.
- Bouchard, M., Pothier, D., 2010. Spatiotemporal variability in tree and stand mortality caused by spruce budworm outbreaks in eastern Quebec. *Can. J. For. Res.* 40, 86–94.
- Boulanger, Y., Arseneault, D., 2004. Spruce budworm outbreaks in eastern Quebec over the last 450 years. *Can. J. For. Res.* 34, 1035-1043.
- Boulanger, Y., Arseneault, D., Morin, H., Jardon, Y., Bertrand, P., Dagneau, C., 2012. Dendrochronological reconstruction of spruce budworm (*Choristoneura fumiferana*) outbreaks in southern Quebec for the last 400 years. *Can. J. For. Res.* 42, 1264-1276.
- Boulet, B., Chabot, M., Dorais, L., Dupot, A., Gagnon, R., 1996. Entomologie forestière. Dans *Manuelle de foresterie*. Sous la direction de Bérard, J.A., Côté, M., Les Presses de l'Université Laval, Québec, pp. 1008-1043.
- Briffa, K.R., 1995. Statistical aspects of the interpretation of high-resolution proxy climate data: the example of dendroclimatology. In: Von Storch, H. Navarra, A. (eds.), *Analysis of climate variability: applications of statistical techniques*, Springer, Berlin, pp. 77-94.
- Candau, J-N., Fleming, R.A., 2011. Forecasting the response of spruce budworm defoliation to climate change in Ontario. *Can. J. For. Res.* 41, 1948-1960.
- Centritto, M., Tognetti, R., Leitgeb, E., Štřelcová, K., Cohen, S., 2011. Above ground processes - anticipating climate change influences. In: Bredemeier, M., Cohen, S., Godbold, D., Lode, E., Pichler, V., Schleppi, P. (eds.), *Forest management and the water cycle*, Springer, Berlin, Ecological Studies 212: 31–64.
- Christensen, J.H., Carter, T.R., Rummukainen, M., Amanatidis, G., 2007. Evaluating the performance and utility of regional climate models: The PRUDENCE project. *Climatic Change* 81(Suppl.), 1–6.

464 Coccozza, C., Giovannelli, A., Lasserre, B., Cantini, C., Lombardi, F., Tognetti, R., 2012. A
 465 novel mathematical procedure to interpret the stem radius variation in olive trees. *Agric. For.*
 466 *Meteorol.* 161, 80-93.

467 Cook, E.R., Briffa, K., Shiyatov, S., Mazepa, V., 1990. Tree standardization and growth-trend
 468 estimation. In: Cook, E.R., Kairiukstis, L. (eds.), *Methods of dendrochronology*, Kluwer,
 469 Amsterdam, pp. 104-132.

470 Cooke, B.J., Roland, J., 2007. Trembling aspen responses to drought and defoliation by forest
 471 tent caterpillar and reconstruction of recent outbreaks in Ontario. *Can. J. Forest Res.* 37, 1586-
 472 1598.

473 D'Arrigo, R., Wilson, R., Liepert, B., Cherubini, P., 2008. On the 'divergence problem' in
 474 Northern forests: a review of the tree-ring evidence and possible causes. *Glob. Planet. Change*
 475 60, 289–305.

476 Direction de la protection des forêts, 2012. Aires infestées par la tordeuse des bourgeons de
 477 l'épinette au Québec en 2012. In: MRNF (ed.), *Gouvernement du Québec*, p. 21.

478 Drobyshev, I., Gewehr, S., Berninger, F., Bergeron, Y., 2013. Species specific growth
 479 responses of black spruce and trembling aspen may enhance resilience of boreal forest to
 480 climate change. *J. Ecol.* 101, 231-242.

481 Genries, A., Drobyshev, I., Bergeron, Y., 2012. Growth-climate response of jack pine on clay
 482 soils in northeastern Canada. *Dendrochronologia* 30, 127-136.

483 Goodine, G.K., Lavigne, M.B., Krasowski, M.J., 2008. Springtime resumption of
 484 photosynthesis in balsam fir (*Abies balsamea*). *Tree Physiol.* 28, 1069-1076.

485 Gray, D.R., 2008. The relationship between climate and outbreak characteristics of the spruce
 486 budworm in eastern Canada. *Climatic Change* 87, 361–383.

487 Gričar, J., Zupančič, M., Čufar, K., Oven, P., 2007. Regular cambial activity and xylem and
 488 phloem formation in locally heated and cooled stem portions of Norway spruce. *Wood Sci.*
 489 *Technol.* 41, 463 – 475.

490 Han, E.N., Bause, E., 2000. Dormancy in the life cycle of the spruce budworm: physiological
 491 mechanisms and ecological implications. *Rec. Res. Dev. Entomol.* 3, 43–54.

492 Huang, J.-G., Bergeron, Y., Berninger, F., Zhai, L., Tardif, J.C., et al., 2013. Impact of future
 493 climate on radial growth of four major boreal tree species in the eastern Canadian boreal forest.
 494 *PLoS ONE* 8, e56758.

495 Huang, J.G., Tardif, J., Denneler, B., Bergeron, Y., Berninger, F., 2008. Tree-ring evidence
 496 extends the historic northern range limit of severe defoliation by insects in the aspen stands of
 497 western Quebec, Canada. *Can. J. For. Res.* 38, 2535–2544.

498 Jardon, Y., Morin, H., Dutilleul, P., 2003. Périodicité et synchronisme des épidémies de la
 499 tordeuse des bourgeons de l'épinette au Québec. *Can. J. For. Res.* 33, 1947–1961.

500 Jobidon, R., Bergeron, Y., Robitaille, A., Raulier, F., Gauthier, S., Imbeau, L., Saucier, J.-P.,
 501 Boudreault, C., 2015. A biophysical approach to delineate a northern limit to commercial
 502 forestry: the case of Quebec's boreal forest. *Can. J. For. Res.* 45, 515–528.

503 Kaennel, K., Schweingruber, F.H., 1995. Multilingual glossary of dendrochronology. Terms
 504 and definitions in English, German, French, Spanish, Italian, Portuguese, and Russian. Swiss
 505 Federal Institute for Forest, Snow and Landscape Research, Birmensdorf. Paul Haupt
 506 Publishers, Berne, p. 467.

507 Kneeshaw, D., Bergeron, Y., Kuuluvainen, T., 2011. Forest ecosystem dynamics across the
 508 circumboreal forest. In: Millington, A.C., Blumler, M.A., MacDonald, G., Shickhoff, U.,
 509 (eds.), *Handbook of biogeography*, Sage, Washington, Chapter 14, pp. 261–268.

510 Ko Heinrichs, D., Tardif, J.C., Bergeron, Y., 2007. Xylem production in six tree species
 511 growing on an island in the boreal forest region of western Quebec. Canada. *Can. J. Bot.* 85,
 512 518-525.

513 Krause, C., Luszczynski, B., Morin, H., Rossi, S., Plourde, P.Y., 2012. Timing of growth
 514 reductions in black spruce stem and branches during the 1970s spruce budworm outbreak. *Can.*
 515 *J. For. Res.* 42, 1220–1227.

516 Krause, C., Rossi, S., Thibeault-Martel, M., Plourde, P.-Y., 2010. Relationships of climate and
 517 cell features in stems and roots of black spruce and balsam fir. *Ann. For. Sci.* 67, 402.

518 Kruskal, W.H., Wallis, W.A., 1952. Use of ranks in one criterion variance analysis. *J. Am. Stat.*
 519 *Ass.* 47, 583-621.

520 Lugo, J.L., Deslauriers, A., Rossi, S., 2012. Duration of xylogenesis in black spruce lengthened
 521 between 1950 and 2010. *Ann. Bot.* 110, 1099-1108.

522 McLeod, A.I., 2013. Kendall rank correlation and Mann-Kendall trend test, Package 'Kendall',
 523 CRAN R statistical software.

524 Pureswaran, D.S., De Grandpré, L., Paré, D., Taylor, A., Barrette, M., Morin, H., Régnière, J.,
 525 Kneeshaw, D.D., in press. Climate-induced changes in host tree-insect phenology may drive
 526 ecological state-shift in boreal forest. *Ecology*. <http://dx.doi.org/10.1890/13-2366.1>.

527 Régnière, J., Saint-Amant, R., Bechard, A., 2014. *BioSIM 10 – User's Manual*. Natural
 528 Resources Canada, Canadian Forest Service, Laurentian Forestry Centre, Québec, Canada.

529 Régnière, J., St. Amant, R., Duval, P., 2012. Predicting insect distributions under climate
 530 change from physiological response: spruce budworm as an example. *Biol. Invasions* 14, 1571-
 531 1586.

532 Régnière, J., St-Amant, R., 2007. Stochastic simulation of daily air temperature and
 533 precipitation from monthly normals in North America north of Mexico. *Int. J. Biometeorol.* 51,
 534 415–430.

535 Rossi S., Deslauriers A., Anfodillo T., Carraro V. (2007) Evidence of threshold temperatures
 536 for xylogenesis in conifers at high altitudes. *Oecologia* 152, 1–12.

537 Rossi, S., Girard, M.-J., Morin, H., 2014. Lengthening of the duration of xylogenesis engenders
 538 disproportionate increases in xylem production. *Glob. Change Biol.* 20, 2261–2271.

539 Rossi, S., Morin, H., Deslauriers, A., Plourde, P.Y., 2011. Predicting xylem phenology in black
 540 spruce under climate warming. *Glob. Change Biol.* 17, 614–625.

541 Shlichta, J.G., Smilanich, A.M., 2012. Immune responses and their potential role in insect
 542 outbreaks. In: Barbosa, P., Letourneau, D.K., Agrawal, A.A. (eds.), *Insect outbreaks revisited*,
 543 Blackwell Publishing Ltd., pp. 47–70.

544 Silva, L.C.R., Anand, M., Leithead, M.D., 2010. Recent widespread tree growth decline despite
 545 increasing atmospheric CO₂. *PLoS ONE* 5, e11543.

546 Simard, S., Elhani, S., Morin, H., Krause C., Cherubini, P., 2008. Carbon and oxygen stable
 547 isotopes from tree-rings to identify spruce budworm outbreaks in the boreal forest of Québec.
 548 *Chem. Geol.* 252, 80–87

549 Simard, S., Morin, H., Krause, C., 2011. Long-term spruce budworm outbreak dynamics
 550 reconstructed from subfossil trees. *J. Quatern. Sci.* 26, 734–738.

551 Simard, S., Morin, H., Krause, C., Buhay, W.M., Treydte, K., 2012. Tree-ring widths and
 552 isotopes of artificial defoliated balsam firs: A simulation of spruce budworm outbreaks in
 553 Eastern Canada. *Env. Exp. Bot.* 81, 44–54.

554 Sturtevant, B.R., Achtemeier, G.L., Charney, J.J., Anderson, D.P., Cooke, B.J., Townsend,
 555 P.A., 2013. Long-distance dispersal of spruce budworm (*Choristoneura fumiferana* Clemens)
 556 in Minnesota (USA) and Ontario (Canada) via the atmospheric pathway. *Agric. For. Meteorol.*
 557 168, 186– 200.

558 Tanja, S., Berninger, F., Vesala, T., Markkanen, T., Hari, P., Mäkelä, A., Ilvesniemi, H.,
 559 Hänninen, H., Nikinmaa, E., Huttula, T., Laurila, T., Aurela, M., Grelle, A., Lindroth, A.,
 560 Arneth, A., Shibistova, O., Lloyd, J., 2003. Air temperature triggers the recovery of evergreen
 561 boreal forest photosynthesis in spring. *Glob. Change Biol.* 9, 1410–1426.

562 Tognetti, R., Lombardi, F., Lasserre, B., Cherubini, P., Marchetti, M., 2014. Tree-ring stable
 563 isotopes reveal twentieth-century increases in water-use efficiency of *Fagus sylvatica* and
 564 *Nothofagus* spp. in Italian and Chilean mountains. *PLoS ONE* 9, e113136.

565 Tremblay, M.J., Rossi, S., Morin, H., 2011. Growth dynamics of black spruce in stands located
566 between the 51st and 52nd parallels in the boreal forest of Quebec, Canada. *Can. J. For. Res.*
567 41, 1769-1778.

568 Wigley, T.M.L., Briffa, K.R., Jones, P.D., 1984. One the average value of correlated time
569 series, with applications in dendroclimatology and hydrometeorology. *J. Appl. Meteorol. Clim.*
570 23, 201 -213.

571 Williams, D.W., Liebhold, A.M., 2000. Spatial synchrony of spruce budworm outbreaks in
572 eastern North America. *Ecology* 81, 2753–2766.

573 Zang, C., Biondi, F., 2013. Dendroclimatic calibration in R: the bootRes package for response
574 and correlation function analysis. *Dendrocronologia* 31, 68-74.

575 Zhang, X., Lei, Y., Ma, Z., Kneeshaw, D., Peng, C., 2014. Insect-induced tree mortality of
576 boreal forests in eastern Canada under a changing climate. *Ecol. Evolut.* 4, 2384–2394.

577

578

579 **Tables**

580 Table 1 – Descriptive statistics for tree-ring chronologies at the sampling sites (SIM, BER, MIS,
 581 DAN). The raw mean ring width and SD were computed on the raw tree ring series; MS, AC, rbar and
 582 EPS were computed on the indexed tree ring series.

DESCRIPTIVE STATISTICS	SIM	BER	MIS	DAN
CHRONOLOGY TIME SPAN (TOTAL YEARS)	1899-2012 (114)	1897-2012 (116)	1901-2012 (110)	1880-2012 (133)
RAW MEAN RING WIDTH (MM)	1.44 (0.89-1.89)	0.67 (0.50-0.99)	0.90 (0.50-1.45)	0.68 (0.50-0.89)
STANDARD DEVIATION (SD)	0.75	0.30	0.52	0.48
MEAN SENSITIVITY (MS)	0.149	0.104	0.125	0.084
FIRST-ORDER SERIAL AUTOCORRELATION (AC)	0.162	0.409	0.473	0.380
MEAN INTER- SERIES CORRELATION (RBAR)	0.433	0.351	0.515	0.205
MEAN EXPRESSED POPULATION SIGNAL – (MEAN EPS) (NUMBER OF YEARS)	0.831 (6)	0.925 (6)	0.943 (6)	0.836 (7)

583

Table 2 - Statistical values of the cross-timing procedure in non-outbreak and outbreak periods. The Glk (Gleichläufigkeit) is a measure of year-to-year sign of agreement between the interval trend of two chronologies, or the sum of the equal slope intervals as a percentage. Glk is significant, $p < 0.05$, at 62%, and highly significant, $p < 0.01$, at 61%. The GSL is the statistical significance of the Glk significance for the Glk value: * = 95%; ** = 99%. Lag represents the number years of shifts in chronologies (adding or subtracting years from 0 to 5), this procedure was required to obtain the maximum level of Glk and GSL by cross-dating.

		Pc		Tx		Tn		SBW	
non-outbreak		lag (years)	Glk ^{GSL}	lag (years)	Glk ^{GSL}	lag (years)	Glk ^{GSL}	lag (years)	Glk ^{GSL}
1901-1914	SIM	+5	75 ^{ns}	+4	83*	+3	77*	+1	75*
	BER	+4	83*	0	81*	0	73*	+4	72 ^{ns}
	MIS	+4	67 ^{ns}	+5	63 ^{ns}	+4	65 ^{ns}	+2	73 ^{ns}
	DAN	+1	63 ^{ns}	+3	80*	+4	65 ^{ns}	+4	78*
1930-1945	SIM	+3	83*	0	67 ^{ns}	+5	75 ^{ns}	+5	90**
	BER	0	73*	+3	70 ^{ns}	+3	70 ^{ns}	+3	71 ^{ns}
	MIS	+3	75*	0	58 ^{ns}	0	58 ^{ns}	+3	63 ^{ns}
	DAN	+5	70 ^{ns}	0	62 ^{ns}	+5	86*	+3	79*
1960-1973	SIM	+5	81*	+5	75 ^{ns}	+5	75 ^{ns}	+4	67 ^{ns}
	BER	+3	70 ^{ns}	+3	70 ^{ns}	+3	70 ^{ns}	+1	92**
	MIS	+2	64 ^{ns}	0	58 ^{ns}	0	58 ^{ns}	+4	78*
	DAN	+3	70 ^{ns}	0	62 ^{ns}	+5	86*	+4	67 ^{ns}
1989-2004	SIM	+3	71 ^{ns}	+3	67 ^{ns}	+3	71 ^{ns}	+5	90**
	BER	+5	70 ^{ns}	+3	71 ^{ns}	+3	71 ^{ns}	+3	63 ^{ns}
	MIS	+2	62 ^{ns}	+1	57 ^{ns}	+3	71 ^{ns}	0	77*
	DAN	+5	70 ^{ns}	0	67 ^{ns}	+5	70 ^{ns}	+4	73 ^{ns}
		Pc		Tx		Tn		SBW	
outbreak		lag (years)	Glk ^{GSL}	lag (years)	Glk ^{GSL}	lag (years)	Glk ^{GSL}	lag (years)	Glk ^{GSL}
1915-1929	SIM	+2	63 ^{ns}	+5	72 ^{ns}	0	71*	+1	62 ^{ns}
	BER	+4	80*	+3	73 ^{ns}	+3	68 ^{ns}	+3	64 ^{ns}
	MIS	+1	58 ^{ns}	+4	75*	+3	64 ^{ns}	+5	78*

	DAN	+4	75*	+3	77*	+3	82*	+4	75*
1946-1959	SIM	+3	65 ^{ns}	+2	68 ^{ns}	+4	72 ^{ns}	+4	67 ^{ns}
	BER	+5	56 ^{ns}	+5	75 ^{ns}	+1	79*	+5	75 ^{ns}
	MIS	+4	78*	+1	67 ^{ns}	+1	79*	+5	81*
	DAN	+5	81*	0	69 ^{ns}	+2	73 ^{ns}	+1	67 ^{ns}
1974-1988	SIM	+1	65 ^{ns}	0	79*	0	75*	+1	81*
	BER	+4	60 ^{ns}	0	57 ^{ns}	+2	58 ^{ns}	+4	80*
	MIS	+4	70 ^{ns}	0	57 ^{ns}	+3	55 ^{ns}	+4	80*
	DAN	+4	70 ^{ns}	+4	65 ^{ns}	+4	65 ^{ns}	+5	72 ^{ns}

592

























593 Table 3 - Trend series analysis for the complete time interval (1901-2011): Pearson's correlation coefficients between TRI and climatic variables (Pc, Tx and
594 Tn) and SBW (instar pupae frequency); Mann–Kendall rank correlation test of tree ring width (TRW), total precipitation (Pc), mean maximum temperature
595 (Tx), mean minimum temperature (Tn), and insect data, instar pupae frequency (SBW) (S and tau values); Kruskal-Wallis test of TRI between sites for Pc,
596 Tx, Tn, and SBW (instar pupae frequency) (the significance level of the test is 5%) (p-values are shown).

597

SIM				BER				MIS				DAN			
Pearson		correlation coefficient	p-value	correlation coefficient		p-value	correlation coefficient		p-value	correlation coefficient		p-value			
Pc		0.01	0.90	0.14		0.16	-0.20		0.03	0.04		0.69			
Tx		0.20	0.02	0.15		0.13	0.19		0.05	0.25		0.08			
Tn		0.14	0.14	0.10		0.27	0.11		0.25	0.23		0.02			
SBW		-0.18	0.06	0.00		0.97	0.03		0.79	-0.10		0.29			
Kruskal-Wallis		χ²	p-value	χ²		p-value	χ²		p-value	χ²		p-value			
Pc		45.8	0.71	67.8		0.04	45.4		0.66	36.6		0.44			
Tx		56.6	0.31	19.7		0.45	60.4		0.15	40		0.30			
Tn		51.6	0.49	53.5		0.31	56.1		0.26	36.4		0.45			
SBW		56.8	0.30	50.2		0.43	61.4		0.13	33.8		0.57			
Mann Kendhall	tau	S	p-value	tau	S	p-value	tau	S	p-value	tau	S	p-value			
TRW	-0.87	-1174	0.00	-0.74	-4932	0.00	-0.74	-4842	0.00	-0.74	-7581	0.00			
Pc	0.22	1365	0.00	0.40	2447	0.00	0.33	1999	0.00	0.36	1303	0.00			
Tx	0.07	427	0.28	-0.18	-1083	0.01	0.15	925	0.02	0.07	415	0.29			
Tn	0.44	2673	0.00	0.28	1680	0.00	0.32	1945	0.00	0.41	2518	0.00			
SBW	0.22	1303	0.00	0.06	360	0.36	0.06	380	0.33	-0.11	-675	0.09			

598

599 Table 4 – Frequency (expressed in percentage) of climate patterns (expressed by letters), defined by
600 all trend combinations for climatic variables (Pc, Tx, Tn), where arrows refer to trend functions, in
601 CID (complete interval derivative), outbreak and non-outbreak periods.

	Climatic pattern			Synchrony frequency in reference interval		
	Pc	Tx	Tn	CID	outbreak	non-outbreak
A				24%	25%	23%
B				20%	19%	20%
C				5%	6%	5%
D				2%	3%	1%
E				7%	5%	8%
F				20%	21%	19%
G				1%	1%	0%
H				22%	21%	23%

602

Table 5 – Relationships (expressed as frequency in percentage) between TRI and SWB (instar pupae frequency) patterns and most frequent climate patterns (A, B, F, H) in CID, outbreak and non-outbreak periods (patterns with a frequency of more than 30% are expressed in bold). Patterns are defined by arrows for increasing and decreasing trends.

climatic patterns (described in Table 4)		plant-insect patterns			
		TRI ↗ SBW ↗	TRI ↗ SBW ↘	TRI ↘ SBW ↗	TRI ↘ SBW ↘
		synchrony frequency			
		A	B	F	H
		in the complete study interval	in outbreak intervals	in non-outbreak intervals	
A		28%	32%	25%	
B		36%	30%	42%	
F		13%	10%	16%	
H		23%	28%	18%	
	in the complete study interval	15%	43%	17%	
		20%	19%	28%	
		22%	7%	19%	
	in outbreak intervals	35%	37%	35%	
		22%	24%	20%	
	in non-outbreak intervals	26%	26%	20%	
		26%		26%	

Figure captions

Fig. 1 - Map of the study area, with altitude (Alt.), latitude (Lat.) and longitude (Lon.) described for each site.

Fig. 2 – Mean tree-ring width chronologies of black spruce (*Picea mariana* Mill.) trees in four latitudinal plots within the boreal forest of Quebec (SIM is the lowest in latitude, DAN is the highest). The dark gray windows (a), (b) and (c) correspond to outbreaks (1914-1929), (1946-1954) and (1974-1988); the light gray window shows the outbreak still in progress and not yet studied, from 2005 onwards. The white background shows the intervals without outbreak. The reference to 1901 is the starting year of the analysis.

Fig. 3 – Correlation coefficients between tree growth and monthly climatic variables, Pc, Tx and Tn. Correlations were calculated separately for each month for the period from June of the previous year (lowercase letters) to August of the current year (uppercase letters), along the latitudinal transect from SIM to DAN.

Fig. 4 - Derivative trends of tree-growth index (TRI) and instar pupae frequency (SBW) (a), and TRI and mean maximum temperature (Tx) (d) at SIM (as representative of all sites) during the considered period. Details of periods of asynchrony between derivative trends (b), where the time shift of the series is detectable (c), and periods of synchrony between trends (c, e, f), where the overlap of the curves are highlighted.

Fig. 5 – Frequency (expressed in number of cases) of the synchrony per number of consecutive years between derivative values of TRI and Pc, Tx, Tn, and SBW (instar pupae frequency) in each site.